Electronic Supplementary Material (ESI) for Journal of Materials Chemistry A.

Supplementary Materials for

A Multiscale Biomimetic Strategy to Design Strong, Tough Hydrogels by Tuning the Self-assembly Behavior of Cellulose

Yitong Xie[1,2,3†], Shishuai Gao[1,2†], Zhe Ling[2], Chenhuan Lai[2], Yuxiang Huang[5], Jifu Wang[1,2], Chunpeng Wang[1,2], Fuxiang Chu[1,2], Feng Xu[3], Marie-Josée Dumont[4], Daihui Zhang[1,2*]

Affiliations

[1] Institute of Chemical Industry of Forest Products, Chinese Academy of Forestry; National Engineering Laboratory for Biomass Chemical Utilization; Key Laboratory of Chemical Engineering of Forest Products, National Forestry and Grassland Administration; Key Laboratory of Biomass Energy and Material; Nanjing, 210042, Jiangsu, China

[2] Co-Innovation Center of Efficient Processing and Utilization of Forest Resources, Nanjing Forestry University, Nanjing, 210037, Jiangsu, China

[3] College of Materials Science and Technology, Beijing Forestry University, Beijing 100083, China

[4] Department of Bioresource Engineering, McGill University, 21111 Lakeshore Rd., Sainte-Anne-de-Bellevue, QC, Canada

[5] Research Institute of Wood Industry, Chinese Academy of Forestry, No 1 Dongxiaofu, Haidian District, Beijing 100091, China

[*]Corresponding author. Email: Daihui.zhang@mail.mcgill.ca

This PDF file includes:

Supplementary Text
Figs. S1 to S35
Tables S1 to S4
References (1 to 53)

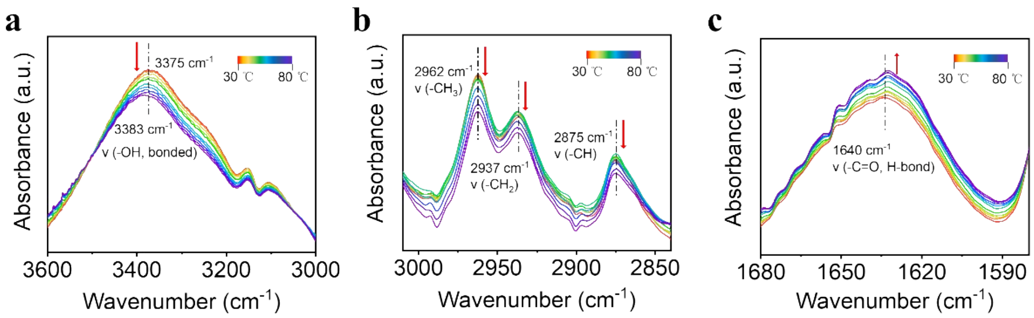

Fig. S1. Temperature-dependent FT-IR spectra of CS-50.

Temperature-dependent FT-IR spectra of CS-50 upon heating from 30 to 80 °C in the wavenumber of 3600 to 3000 cm^{-1} a), 3010 to 2840 cm^{-1} b), and 1680 to 1580 cm^{-1} c).

Fig. S2 Photographs showing the transparency of CS-50.

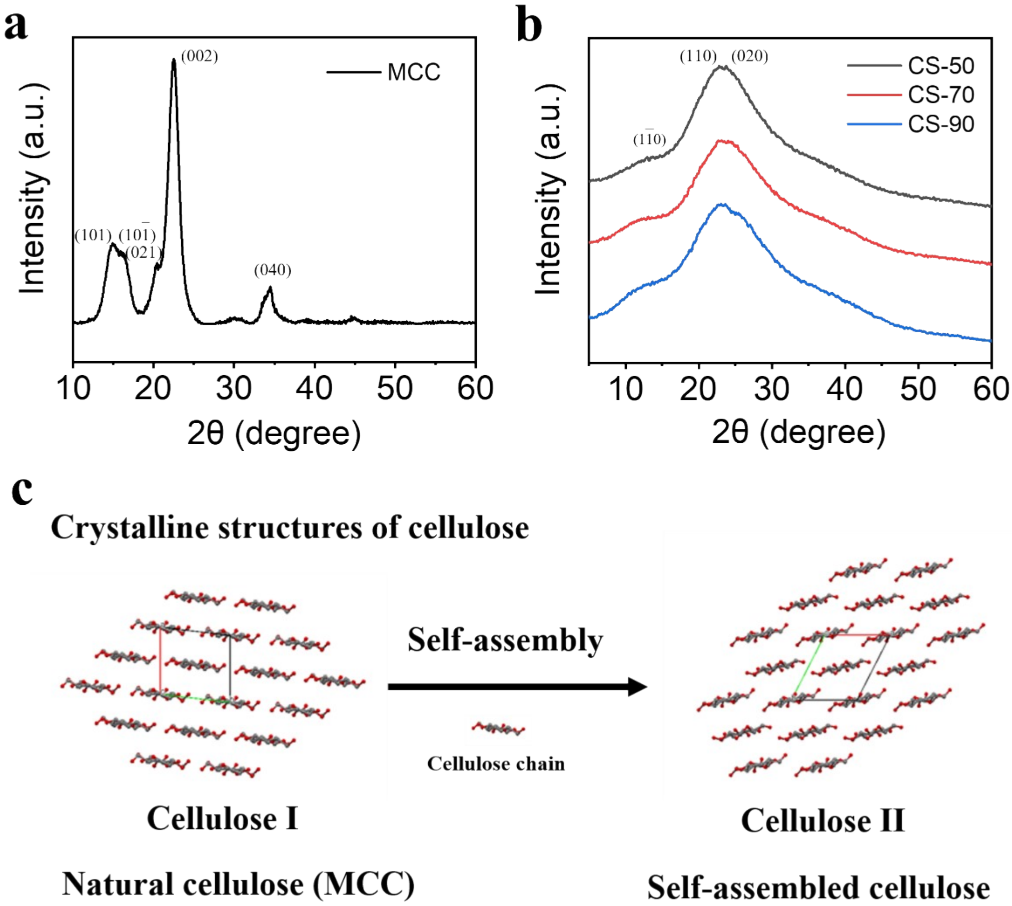

Fig. S3 XRD spectroscopy of MCC a) and CSs b), and c) crystalline structure of cellulose.

XRD analysis showed that as compared to typical diffraction peaks of natural cellulose I crystalline structures which are observed at 2θ=16.5°, 22.5° and 34.8° (Fig. S3a), the characteristic peaks of supramolecular cellulose fibers were observed at 2θ=11.8°, 20.5° and 21.7° (Fig. S3b), indicating the conversion of cellulose I to cellulose II (Fig. S3c).

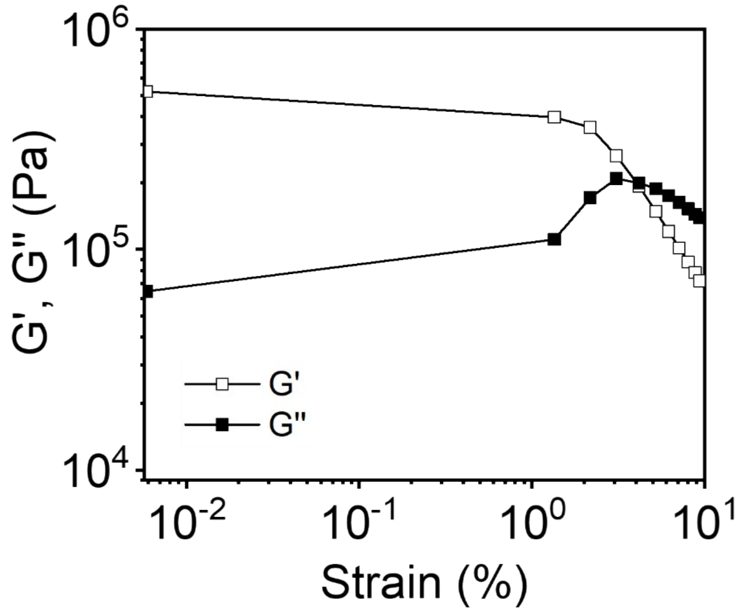

Fig. S4 Complex modulus vs. strain curves for CS-50 at the frequency of 1.00 Hz. Storage (G′) and loss modulus (G″) in linear viscoelastic region (LVR) curve of CS-50 were measured at the strain (γ) range from 0.01% to 100% at an angular frequency of 1 Hz to determine the constant strain (γ) of 1%, which was small enough to avoid the nonlinear response and simultaneously large enough to have a reasonable signal intensity.

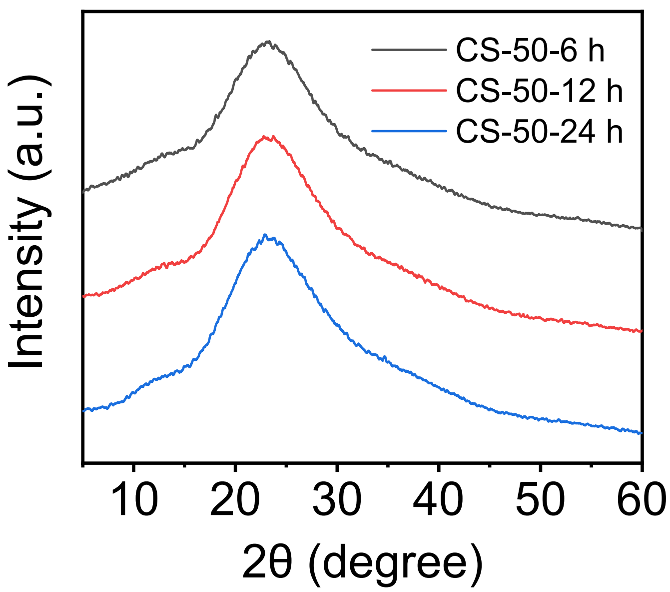

Fig. S5 XRD spectroscopy of CS-50 with different contact duration.

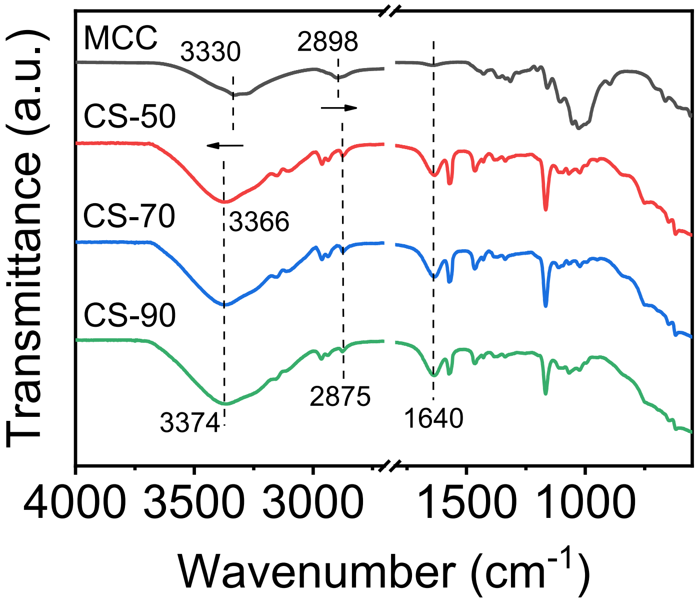

Fig. S6 FT-IR of MCC and CSs in the wavenumber of 4000 to 550 cm^{-1}.

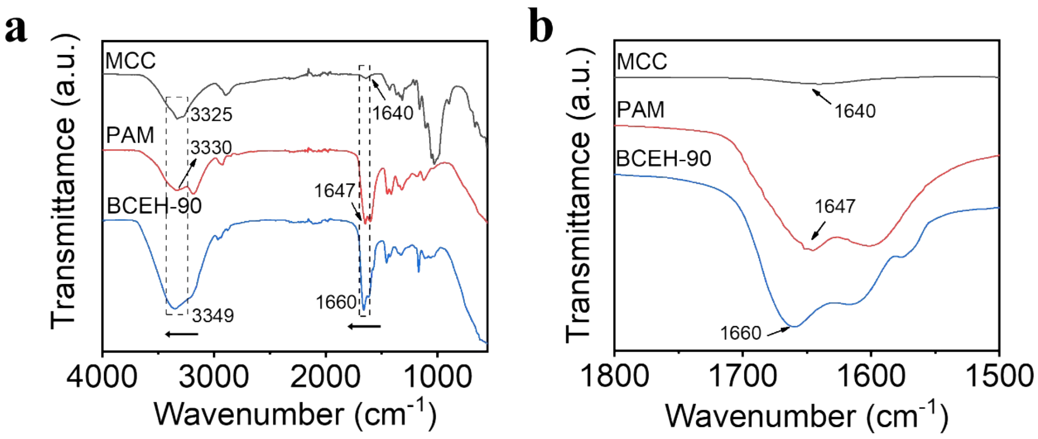

Fig. S7 FT-IR of MCC, PAM, and BCEH-90 in the wavenumber of 4000 to 550 cm^{-1} a) and 1800 to 1500 cm^{-1} b).

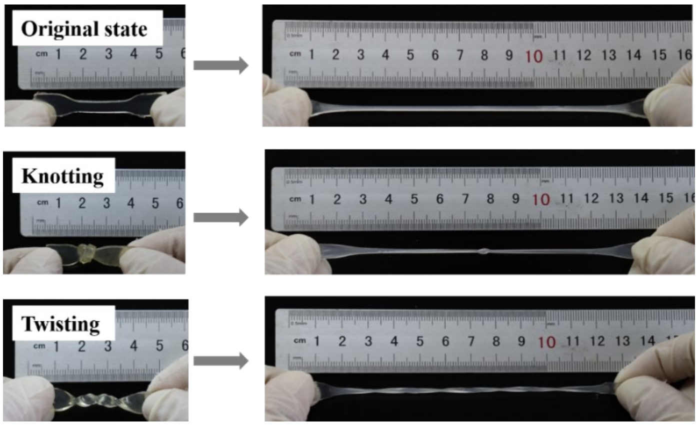

Fig. S8 Stretching, knotting, and twisting of BCEHs.

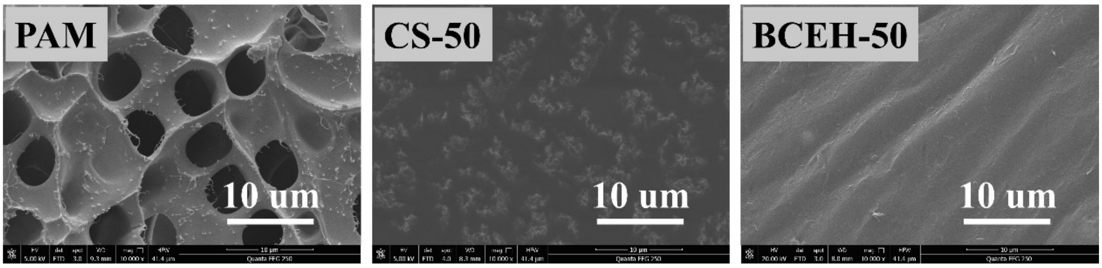

Fig. S9 SEM images of PAM, CS-50, and BCEH-50.

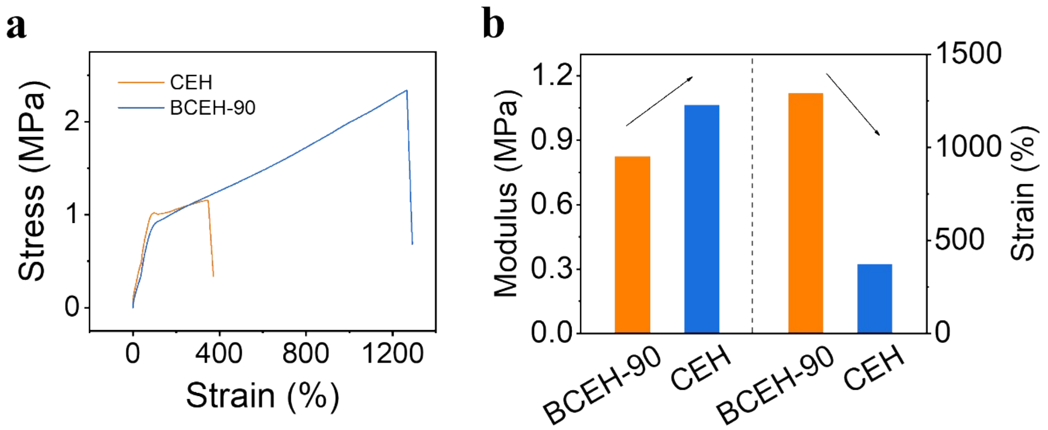

Fig. S10 Mechanical properties of cellulose enhanced hydrogel (CEH) and BCEH-90.

As shown in a and b, the CEH exhibited a stretchability of 371.74% with Young's modulus of 1.06 MPa, while BCEH-90 exhibited a stretchability of 1291.0 % with modulus of 0.82 MPa (b). Due to the complete removal of ILs during the formation of CS, high density of physical crosslinking between cellulose was formed, leading to the enhanced Young's modulus.

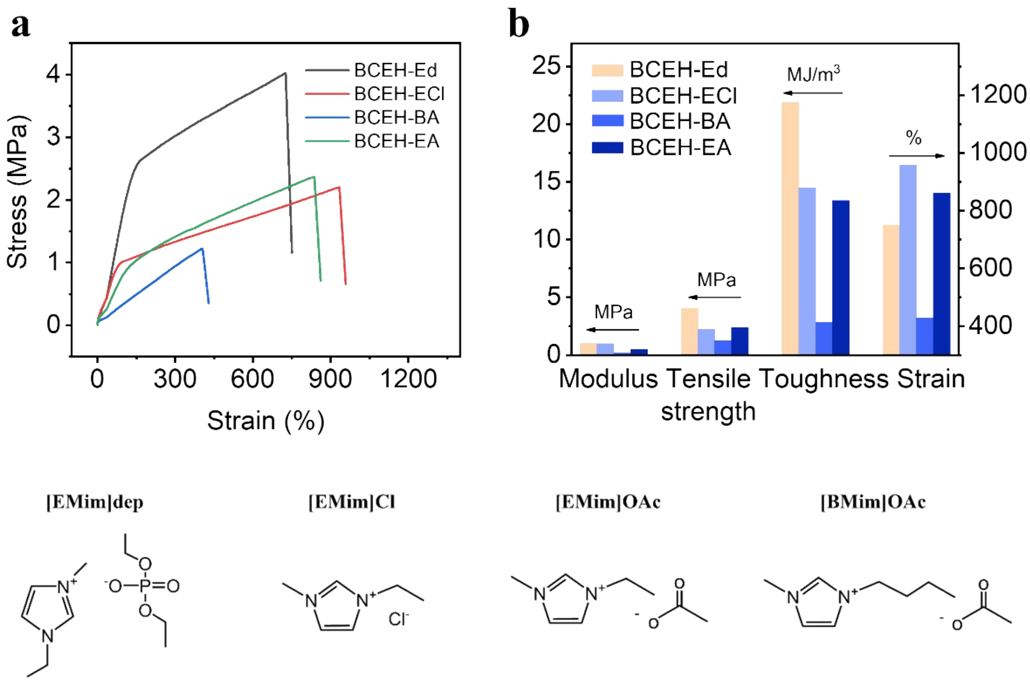

Fig. S11 a) Strain-stress curves of BCEHs; b) Calculated modulus, strength, toughness, and strain of BCEHs.

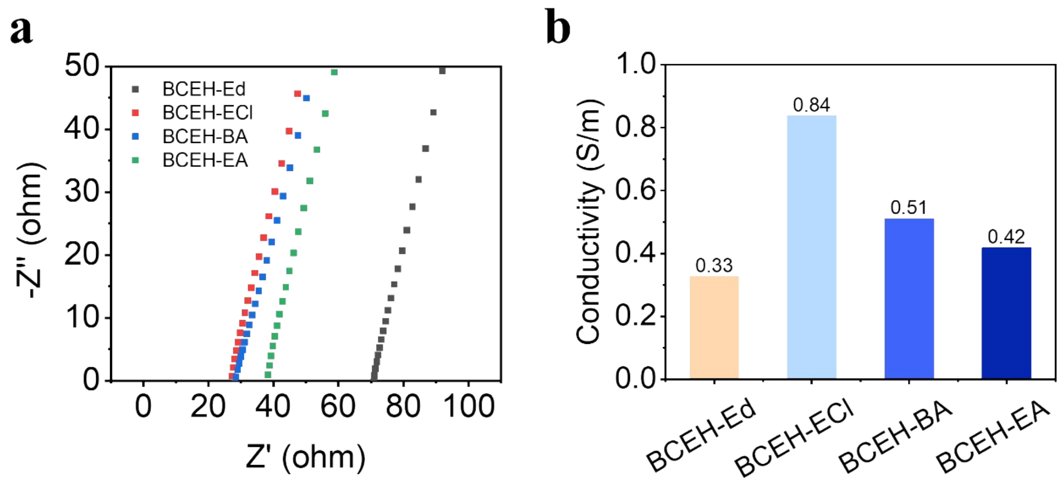

Fig. S12 a) Electrochemical impedance spectroscopy (EIS) curves of BCEHs; b) conductivity of BCEHs.

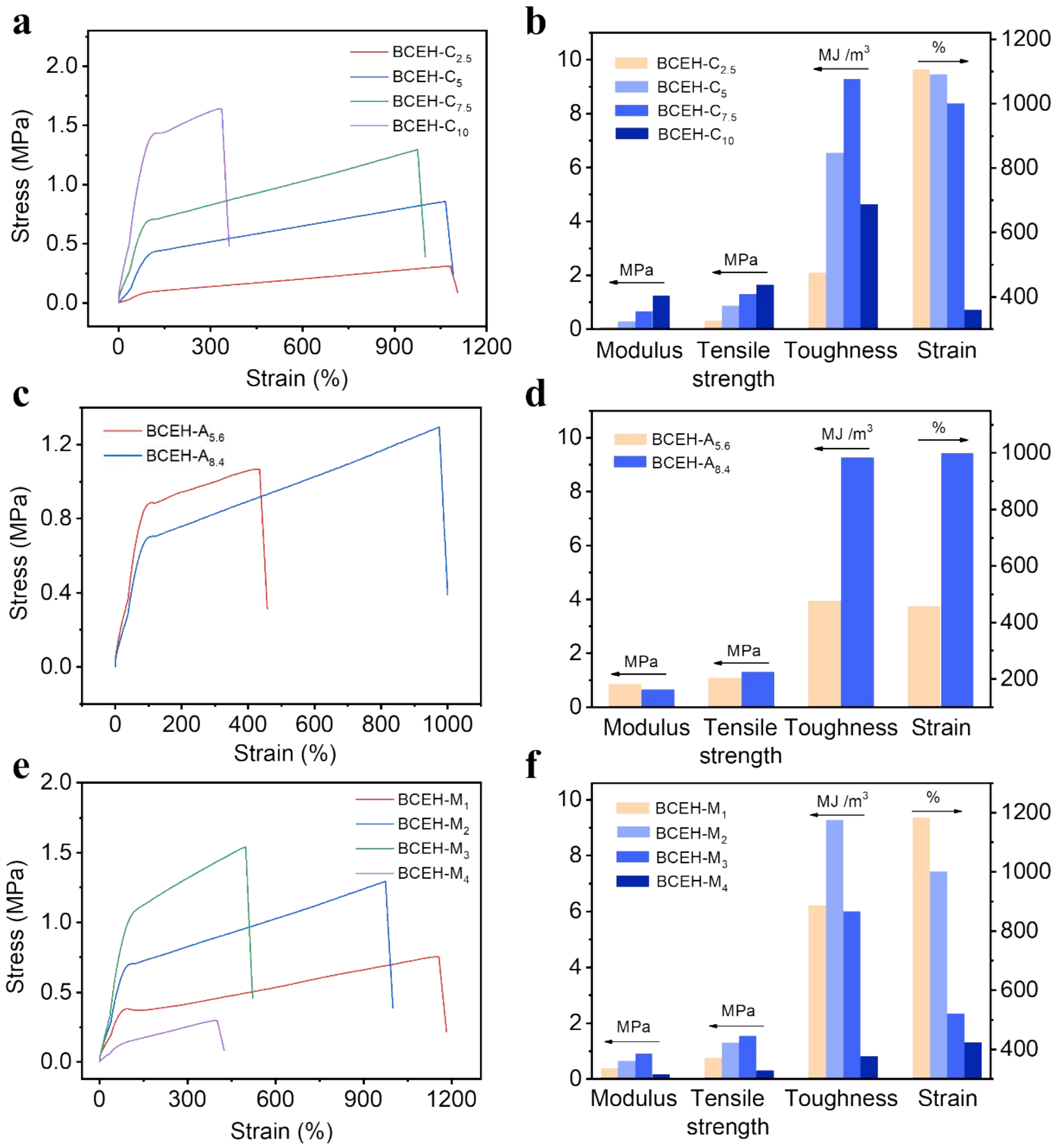

Fig. S13 Effect of cellulose content (a, b), AM concentration (c, d), and MBA content (e, f) on the mechanical properties of BCEHs. BCEH-$C_{2.5}$, C_5 and $C_{7.5}$ and C_{10} indicate that the cellulose concentration was 2.5 wt%, 5.0 wt%, 7.5 wt% and 10.0 wt%, respectively; BCEH-$A_{5.6}$ and $A_{8.4}$ indicate that the concentration of AM in the immersion solution was 5.6 M and 8.4 M, respectively; BCEH-M_1, M_2, M_3 and M_4 indicate that the molar ratios of MBA to AM were 0.065, 0.13, 0.26 and 0.39 mol %, respectively.

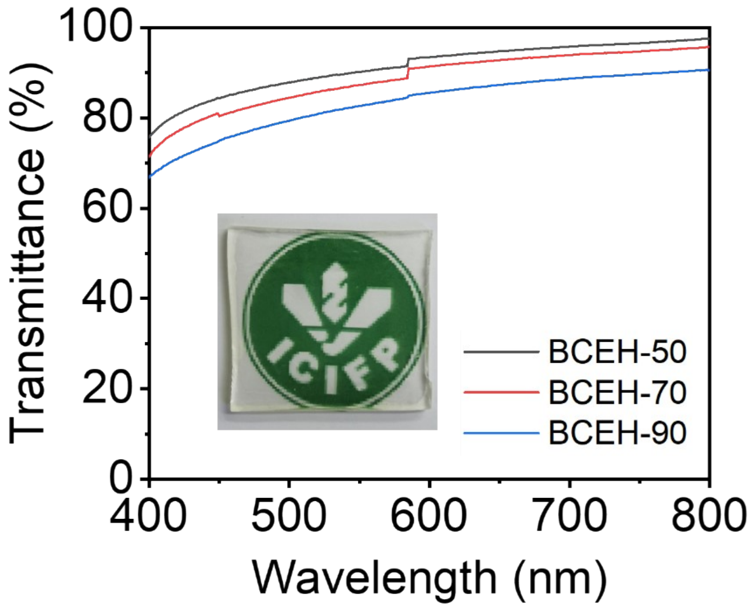

Fig. S14 UV-vis transmittance spectra of BCEHs at wavelength from 400 to 800 nm.

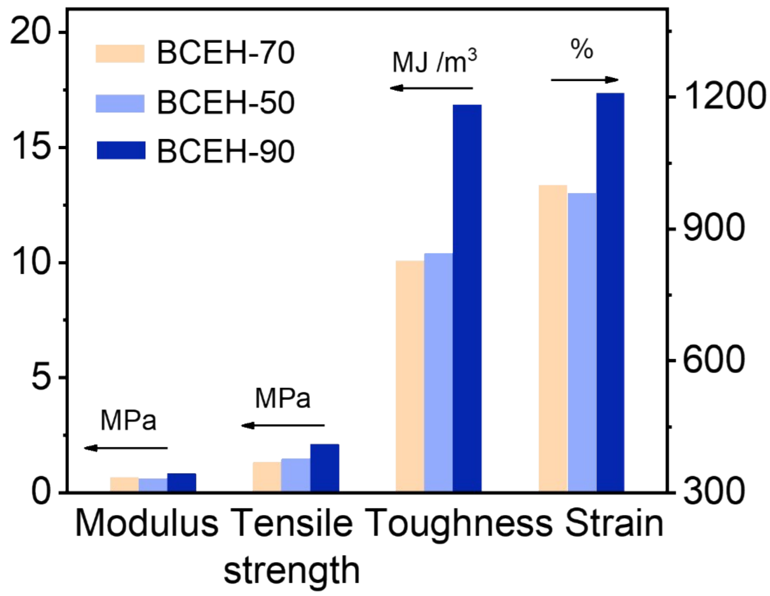

Fig. S15 Calculated modulus, strength, toughness, and strain of BCEHs.

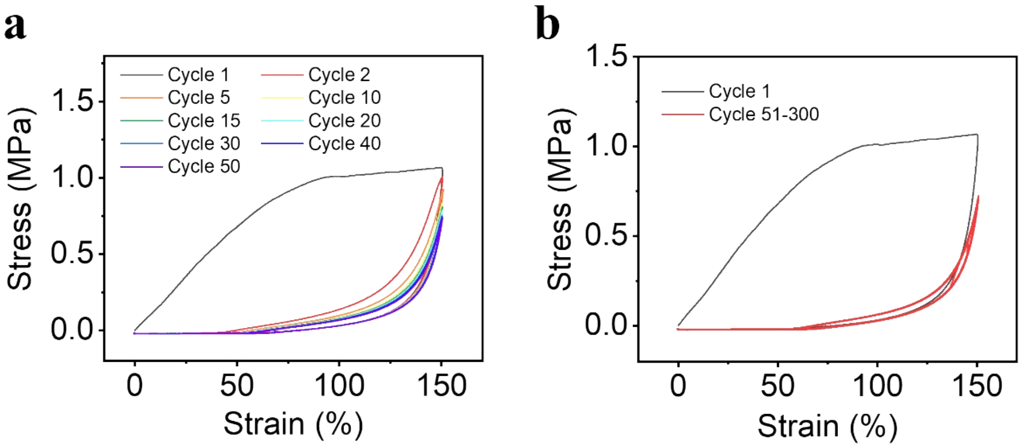

Fig. S16 Tensile test of BCEH-90 in 300 cycles.

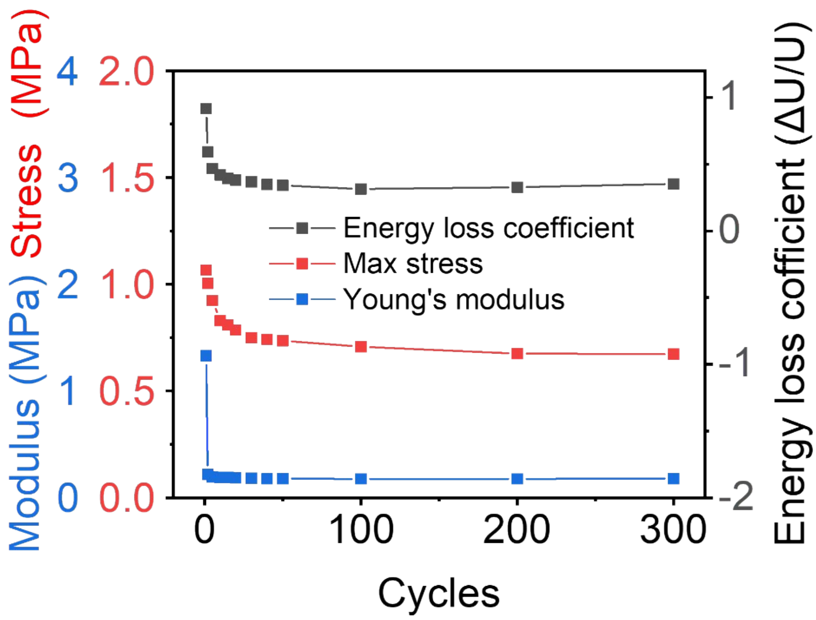

Fig. S17 Young's modulus, maximum stress, and energy loss coefficient versus tensile cycles of BCEH-90.

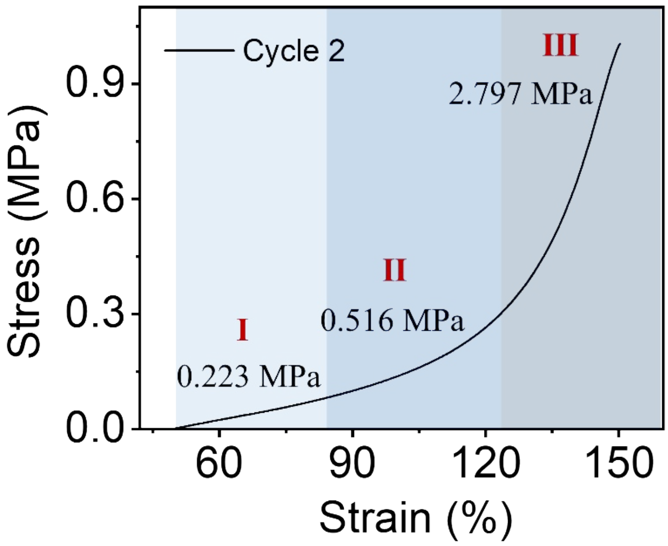

Fig. S18 BCEH-90 exhibited a skin-like non-liner strain-stress behavior.

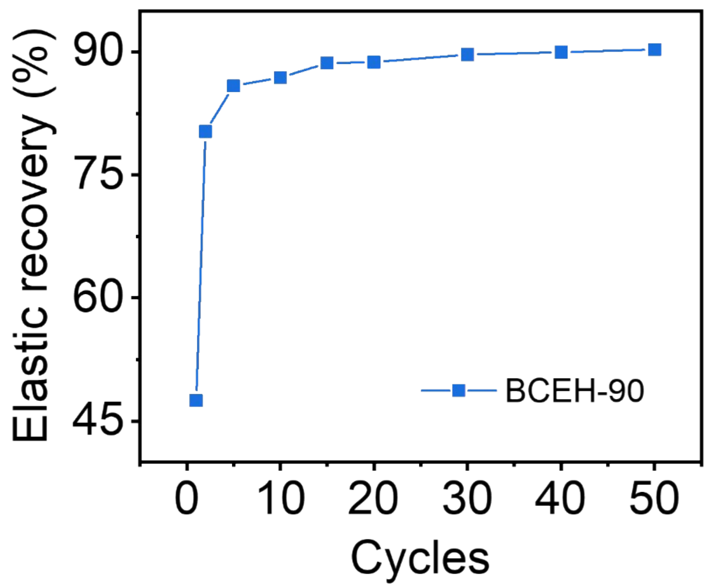

Fig. S19 Elastic recovery of BCEH-90.

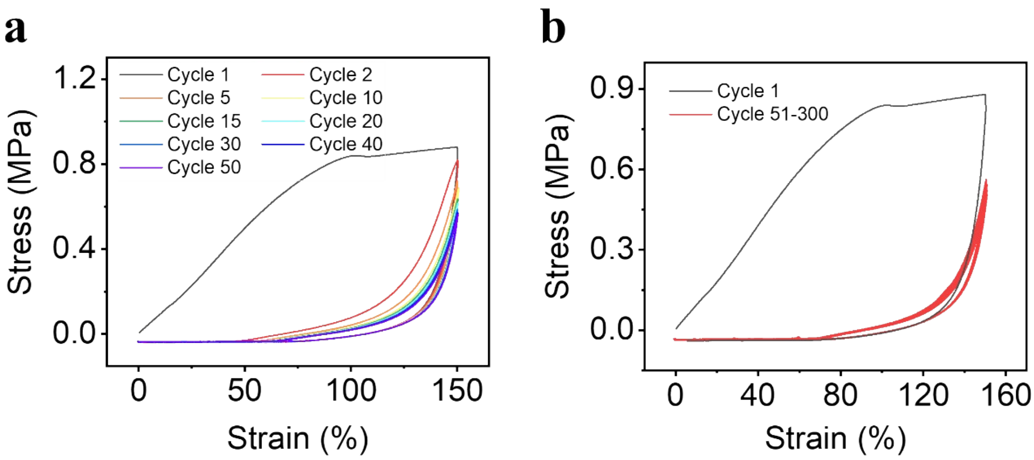

Fig. S20 Tensile test of BCEH-50 in 300 cycles.

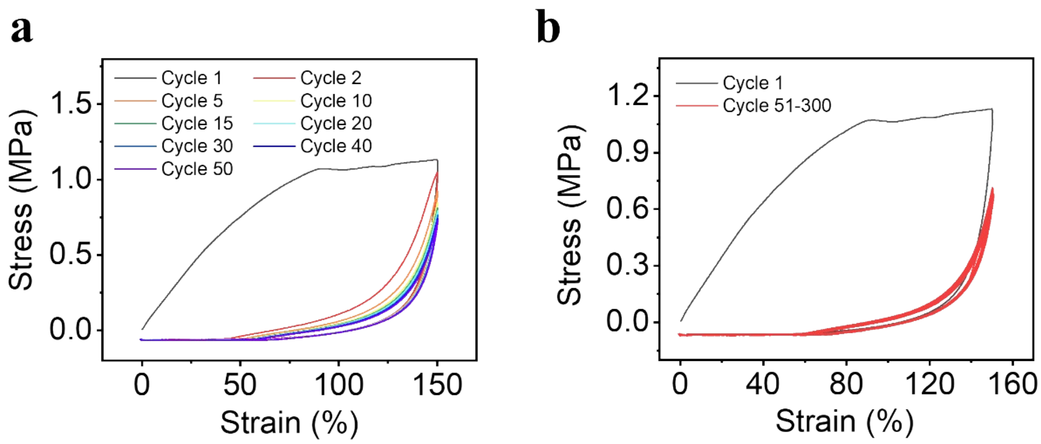

Fig. S21 Tensile test of BCEH-70 in 300 cycles.

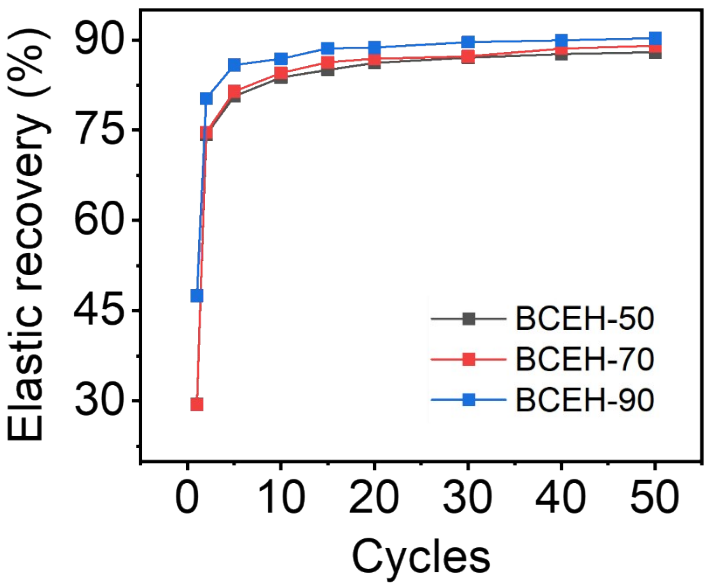

Fig. S22 Elastic recovery of BCEHs during the first 50 tensile test cycles.

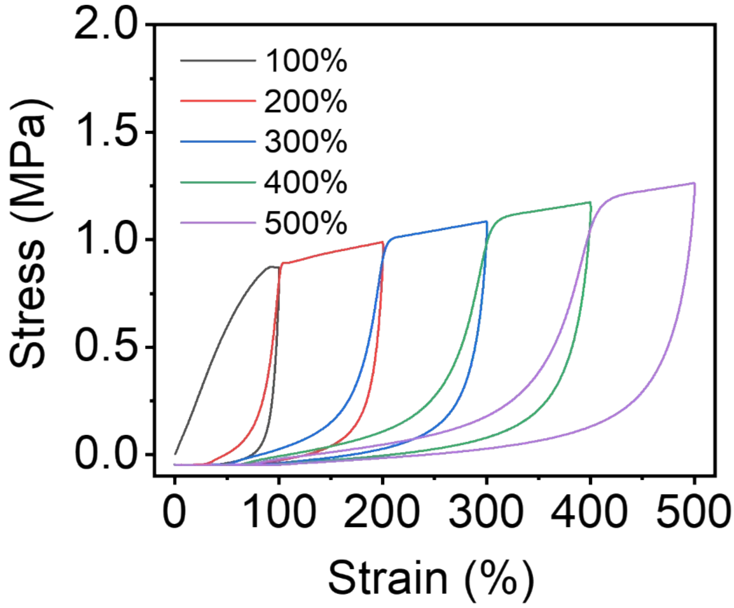

Fig. S23 Loading-unloading curves of BCEH-90 with increased strain from 100% to 500%.

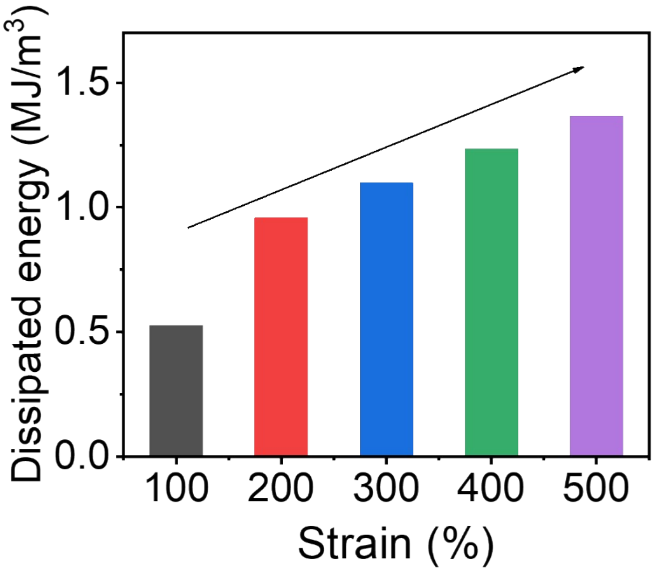

Fig. S24 Dissipation energy of BCEH-90 with increased strain from 100% to 500%.

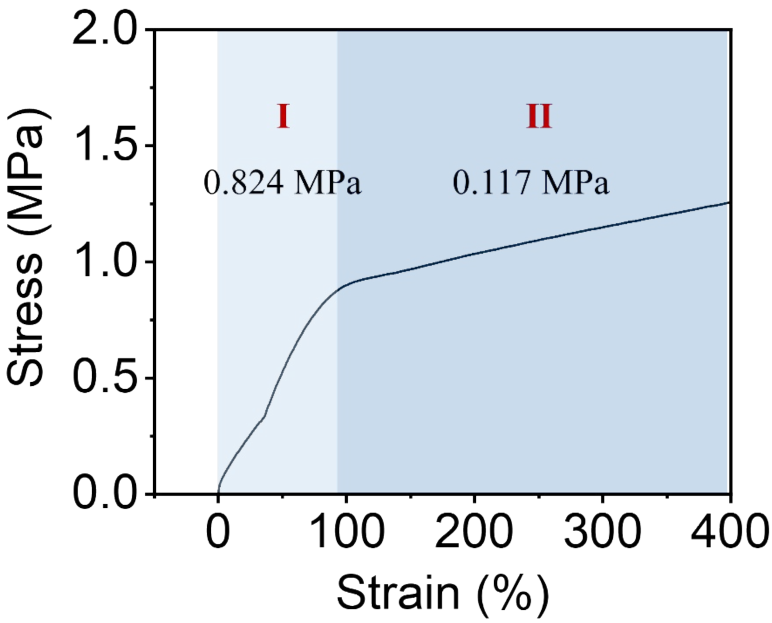

Fig. S25 Two different stages during the stretching process of BCEH-90.

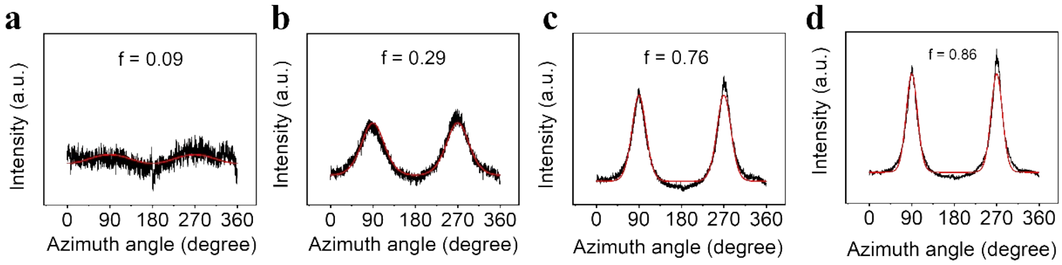

Fig. S26 Typical azimuthal intensity distribution of the SAXS pattern scattering intensity obtained at a strain of a) 0, b) 50%, c) 100%, and d) 300% for BCEH-90. The red curve is the fitting result using the Maier-Saupe distribution function[1].

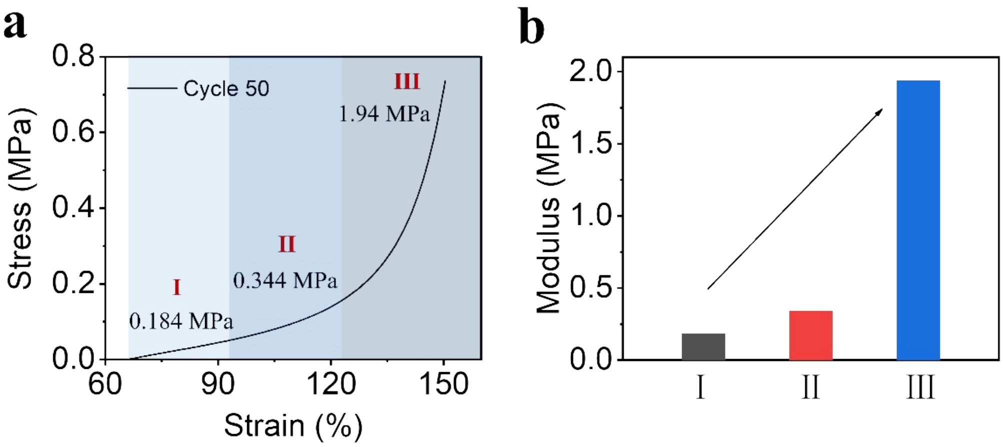

Fig. S27 (a) Dependence of strength on the strain, the cycle 50 curve was divided into three regions depending on the ranges of strain; (b) a gradual increase in the modulus in the 50th cyclic test of BCEH-90.

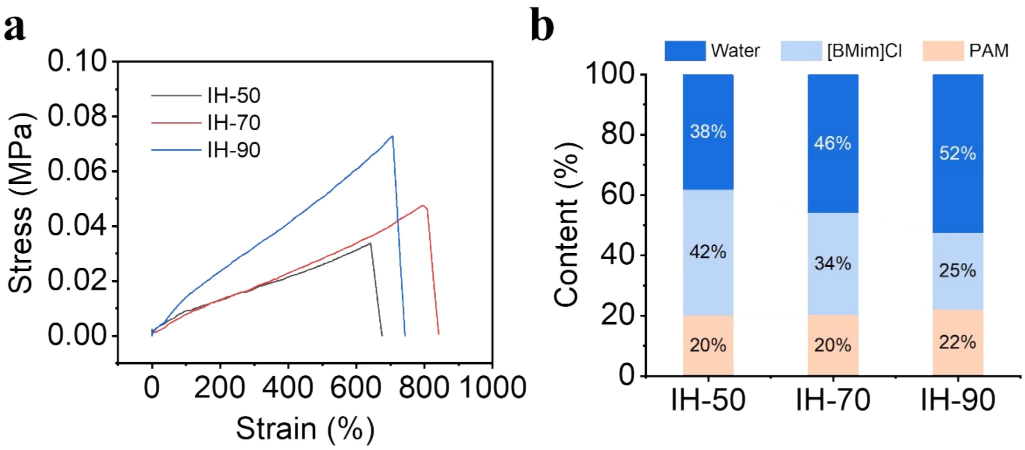

Fig. S28 Tensile tests of IHs (a) and (b) compositions of IHs.

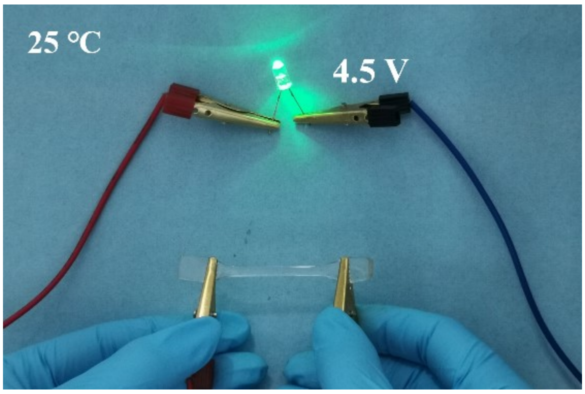

Fig. S29 As a conductor to light a LED bulb at 25 ^{o}C and 4.5 voltage.

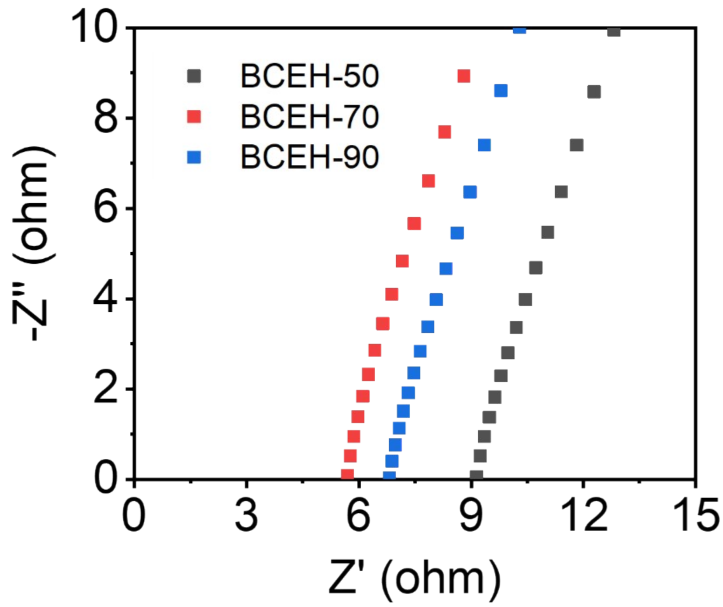

Fig. S30 Electrochemical impedance spectroscopy (EIS) curves of BCEHs.

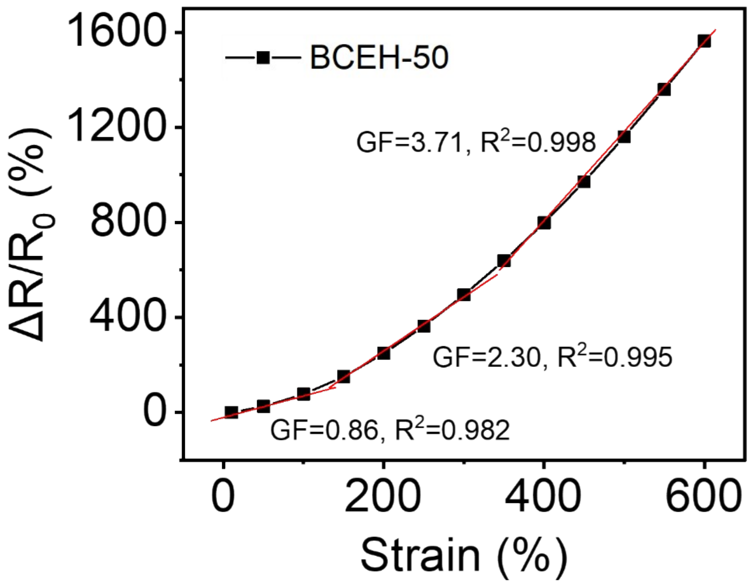

Fig. S31 Gauge factor (GF) of conductive BCEH-50 increases with an increase of strain from 0 to 600%.

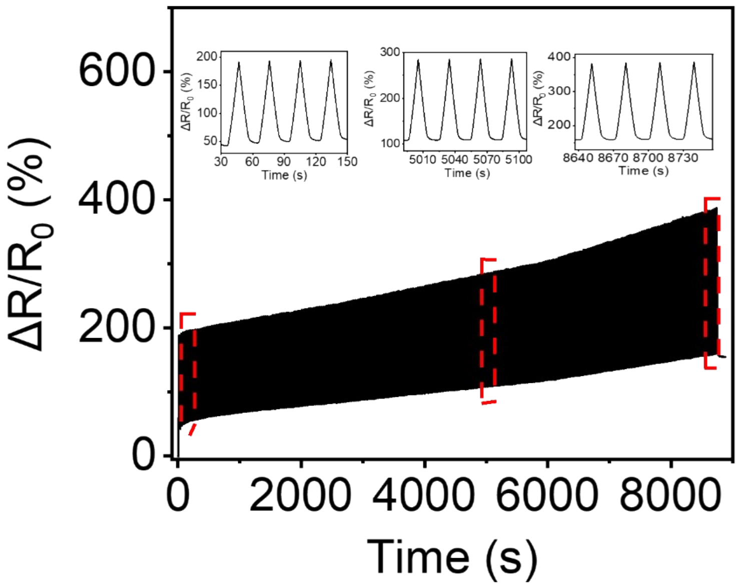

Fig. S32 Cyclic stability tests of BCEH-90 under 150 % strain for 300 cycles

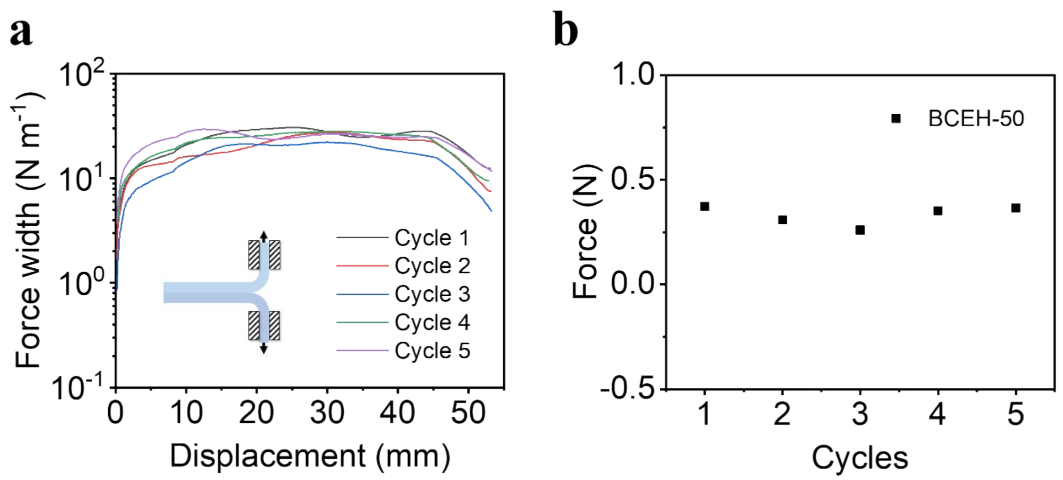

Fig. S33 a) Force/width curve for cycle-adhesion between the BCEH-50; b) 5 times cyclic 180 º peeling tests of BCEH-50.

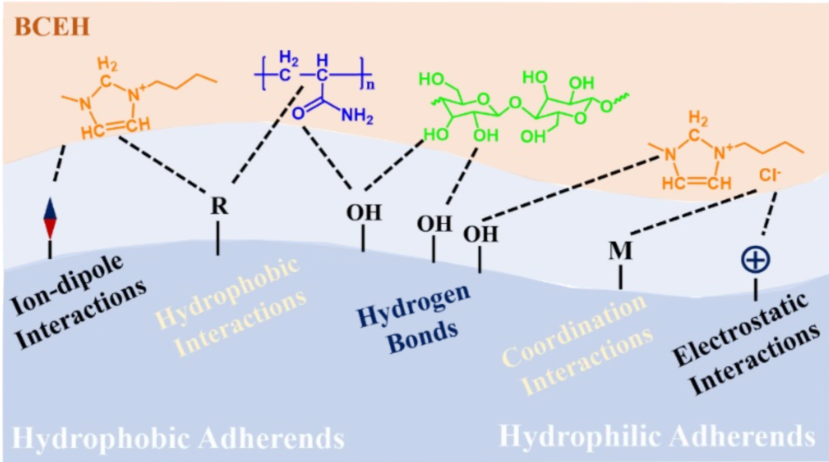

Fig. S34 The adhesive mechanisms between BCEH and adherends.

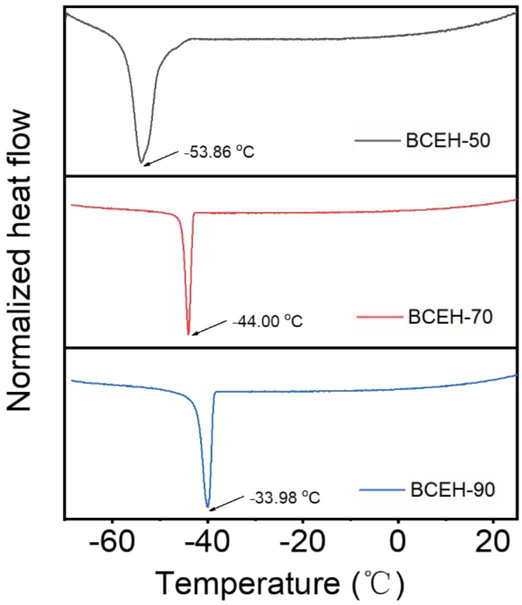

Fig. S35 Differential scanning calorimetry (DSC) curve of BCEHs during the heating process from -70 °C to 25 °C (scan rate 10 °C min^{-1}).

Table S1 Comparison of BCEH-90 with previous strategy of fabricate cellulose enhanced hydrogels

Composition	Type of cellulose	Toughness (MJ/m^3)	Strain (%)	Stress (MPa)	Ref.
BCEH-90	**Cellulose**	**19.5**	**1291**	**2.3**	**This work**
CBH	Cellulose	4.3	900	0.8	[2]
CPH	Cotton linter pulp cellulose	~0.06	747	0.04	[3]
Wood hydrogel	CNF	~1.1 ~2.7	400 14	0.5 36	[4]
A-PDW	CNF	~0.2 ~2.6	57.4±1.7 16.0±1.8	0.7±0.09 16.5±1.4	[5]
BC-PVA-PAMPS	Bacteria cellulose	~1.75	17	20.6	[6]
PAM/CNF	CNF	~1.6	~1200	~0.3	[7]
PVA/CNF	CNF	4.9	660	2.1	[8]
BC/PDES	Bacteria cellulose	~1.92	~290	0.8	[9]
PAM/CMC	CMC	1.0±0.05	2152±70	0.1±0.02	[10]
DCCG	Cotton linter pulp cellulose	1.5	107	2.8	[11]
PANa-cellulose hydrogel	Cellulose	~3.5	1150	~0.6	[12]
CNC-C8 DPC hydrogel	CNC	~4.02	4268±1446	0.3±0.008	[13]
ABCH	Bacteria cellulose	~2.78	38.9±11.2	14.3±2.2	[14]

Table S2 Comparison of BCEH-90 with other hydrogels

Composition	Conductivity (S/m)	Transparency (%)	Toughness (MJ/m^3)	Strain (%)	Tensile strength (MPa)	Ref.
BCEH-90	**1.58**	**86**	**19.42**	**1291**	**2.36**	**This work**
DC-PEO/LiTFSI	0.02	78	~0.74	563	0.26	[15]
CBH	0.30	no	4.3	914	0.8	[2]
Cellulose/PVA	0.46	80 at 550 nm	~0.28	747	0.04	[3]
MEA-AA-graphene	~0.12	no	~1.09	~1250	0.18	[16]
PAAm-oxCNTs	0.07	no	2.29	1041	0.71	[17]

Table S3 Comparison of reported hydrogels with this work

Composition	Strategies	Stress (MPa)	EF	Toughness (MJ/m^3)	EF	Ref.
BCEH-50		**1.30**	**41.37**	**10.07**	**84.97**	
BCEH-70	**Biomimetic**	**1.47**	**32.25**	**10.39**	**56.44**	**This work**
BCEH-90		**2.36**	**25.05**	**19.42**	**47.95**	
Hydrolyzed keratin/ PVA/ NaCl				3.45	74.68	[18]
PAA/CMC$_{1.0}$-Fe^{3+}-S hydrogels				12.06	12.97	[19]
poly (SBMA-coAA)/ LiCl	Salting out	~0.03	~3.57	~0.05	~4.86	
		~0.04	~5.71	~0.12	~11.81	[20]
		~0.058	~8.29	~0.23	~21.81	
PVA/PAM/NaCl		0.48	~1.59	2.48	~1.27	[21]
Agarose/PHEA		0.37	12	~0.79	~18.20	[22]
Agar/ PAAc-Fe^{3+}		0.32	10.67	~3.65	~27.60	[23]
CS-P(AM-co-AA)				15.90	7.23	[24]
PAMPS	DN	0.40	50			[25]
CS-PAAm		0.14	6.14	1.31	8.73	[26]
PAM/CMC/Fe^{3+}		0.90	~15	5.24	~13.97	[10]
SA/PAM/NaCl		0.75	~6.82	4.77	~5.96	[27]
SFRH/NaCl				2.98	3	[28]
MMT/PVA				~2.22	~2.23	[29]
PAA-rGO	Composite	0.40	2	~0.40	~2.79	[30]
CNT-CNF/PVAB		0.05	1.6			[31]
NPs-P-PAA		~0.11	~1.74			[32]
ANFs-PVA		3.30	~4.71			[33]
PSeD-U elastomers		2.42	3	4.59	11	[34]
skin-inspired bilayer hydrogel		0.26	2.43	~1.50	2	[35]
Skin-inspired bilayer composite hydrogel		0.2	5.71	~4.10	~7.32	[36]
P(AAm-co-LMA)/HLPs	Biomimetic	0.74	18.50	5.45	23.08	[37]
				7.83	32.63	
				7.96	33.17	
				8.66	36.08	
				8.99	37.46	
QCS-AMP/PAAm		0.35	3.99	1.46	3.29	[38]

PDA-rGO-PAM		0.15	10			
PAN-PVDF		1.58 1.63 1.72 1.86	1.34 1.38 1.46 1.58			[39]
PVA/EMImAc	Physically crosslinked	~0.32	~3.20	0.60-0.80	~5.71-7.62	[40]
chitosan elastic gel	Oriented	~0.85	~5	~0.17	~1.82	[41]
Alginate-polyacrylamide	Ionically and covalently crosslink	0.16	14.18			[42]
PANi/PA/PVA ItG	ITLP	0.12 0.12	12 12.30	0.10	29	[43]
PVA/PSBMA	Semi-interaction	0.07 0.15 0.23 0.60	2.06 4.78 7.13 18.63	0.60	18	[44]
(RAFT)-modified PAMPS/PAM	Modified first work	0.82	2.24	3.30	2.63-8.51	[45]

Table S4 Comparison of reported natural macromolecules-based hydrogels with this work

Composition	Natural macromolecules	Stress (MPa)	EF	Toughness (MJ/m^3)	EF	Ref.
BCEH-50	**MCC**	**1.30**	**41.37**	**10.07**	**84.97**	**This work**
BCEH-70		**1.47**	**32.25**	**10.39**	**56.44**	
BCEH-90		**2.36**	**25.05**	**19.42**	**47.95**	
PAM/CMC	Carboxymethycellulose	0.14	~2.38	0.98	~2.61	[10]
PVA/CNF	Cellulose nanofibrils	1.40	2.33	5.25	4.09	[8]
		1.70	2.83			
		2.10	3.50	4.90	3.88	
PAM/CNF		~0.27	~3.60	~1.62	~3.32	[46]
BC/PDES	Bacterial cellulose	0.80	4.40	1.92	~14.22	[9]
CS-PAAm	Chitosan	0.14	6.14	1.31	8.73	[26]
PAM-CS		~0.09	3.60	~0.49	5.74	[47]
		~0.15	6	~1.17	13.76	
		~0.12	4.80	~1.28	15	
chitosan elastic gel		~0.85	~5	~0.17	~1.82	[41]
PAA/nano chitin/Al^{3+}		0.40	5.33	~1.58	~3.87	[48]
Agar/PAM	Agar	1	3.33	9	4.74	[49]
Agar/HPAAm		0.27	7.22	9.35	5.40	[50]
Agar/PAMAAc-Fe^{3+}		1.55	2.31	9.13	4.52	[51]
Agar/PAAc-Fe^{3+}		0.32	10.67	~3.65	~27.6	[23]
Agarose/PHEA	Agarose	0.37	12	~0.79	~18.20	[22]
SA nanofibrillar/PAM/NaCl	Sodium alginate	0.75	~6.82	4.77	~5.96	[27]
SA/AAm/AAc				25.10	23.80	[52]
PVA/ferritin	ferritin	~12.15	2.70	~38.7	~12.38	[53]
Wood hydrogel	wood	0.54	7.50	~1.08	4.29	[4]
		36	500	~2.70	10.71	
PDW				~0.16	65.20	[5]
				~0.21	82.40	
				~2.63	1052	

Supplementary references

[1] S. Feng, X. Xiong, G. Zhang, N. Xia, Y. Chen, W. Wang, *Macromolecules* **2009**, 42, 281.

[2] D. Zhang, J. Jian, Y. Xie, S. Gao, Z. Ling, C. Lai, J. Wang, C. Wang, F. Chu, M.-J. Dumont, *Chem. Eng. J.* **2022**, 427, 130921.

[3] Y. Wang, L. Zhang, A. Lu, *Journal of Materials Chemistry A* **2020**, 8, 13935.

[4] W. Kong, C. Wang, C. Jia, Y. Kuang, G. Pastel, C. Chen, G. Chen, S. He, H. Huang, J. Zhang, S. Wang, L. Hu, *Advanced materials* **2018**, 30, e1801934.

[5] C. Chen, Y. Wang, Q. Wu, Z. Wan, D. Li, Y. Jin, *Chemical Engineering Journal* **2020**, 400, 125876.

[6] F. Yang, J. Zhao, W. J. Koshut, J. Watt, J. C. Riboh, K. Gall, B. J. Wiley, *Advanced Functional Materials* **2020**, 30, 2003451.

[7] W. Ge, S. Cao, Y. Yang, O. J. Rojas, X. Wang, *Chemical Engineering Journal* **2020**, 127306.

[8] Y. Z. Yuhang Ye, Yuan Chen, Xiaoshuai Han, Feng Jiang, *AFM* **2020**.

[9] M. Wang, R. Li, X. Feng, C. Dang, F. Dai, X. Yin, M. He, D. Liu, H. Qi, *ACS Appl Mater Interfaces* **2020**, 12, 27545.

[10] Y. Cheng, X. Ren, G. Gao, L. Duan, *Carbohydr Polym* **2019**, 223, 115051.

[11] P. Wei, L. Wang, F. Xie, J. Cai, *Chemical Engineering Journal* **2022**, 431, 133964.

[12] L. Ma, S. Chen, D. Wang, Q. Yang, F. Mo, G. Liang, N. Li, H. Zhang, J. A. Zapien, C. Zhi, *Advanced Energy Materials* **2019**, 9, 1803046.

[13] X. Liu, X. He, B. Yang, L. Lai, N. Chen, J. Hu, Q. Lu, *Advanced Functional Materials* **2021**, 31, 2008187.

[14] M. Zhang, S. Chen, N. Sheng, B. Wang, Z. Wu, Q. Liang, H. Wang, *Nanoscale* **2021**, 13, 8126.

[15] P. Zhang, W. Guo, Z. H. Guo, Y. Ma, L. Gao, Z. Cong, X. J. Zhao, L. Qiao, X. Pu, Z. L. Wang, *Advanced materials* **2021**, e2101396.

[16] X. Liu, Q. Zhang, G. Gao, *ACS Nano* **2020**, 14, 13709.

[17] X. Sun, Z. Qin, L. Ye, H. Zhang, Q. Yu, X. Wu, J. Li, F. Yao, *Chem. Eng. J.* **2020**, 382, 122832.

[18] S. G. Yang Gao, Fei Jia, Guanghui Gao, *JMCA* **2020**.

[19] W. Chen, Y. Bu, D. Li, C. Liu, G. Chen, X. Wan, N. Li, *Cellulose* **2019**, 27, 853.

[20] X. Sui, H. Guo, C. Cai, Q. Li, C. Wen, X. Zhang, X. Wang, J. Yang, L. Zhang, *Chemical Engineering Journal* **2021**, 419, 129478.

[21] G. Chen, J. Huang, J. Gu, S. Peng, X. Xiang, K. Chen, X. Yang, L. Guan, X. Jiang, L. Hou, *Journal of Materials Chemistry A* **2020**, 8, 6776.

[22] J. Sun, G. Lu, J. Zhou, Y. Yuan, X. Zhu, J. Nie, *ACS Appl Mater Interfaces* **2020**, 12, 14272.

[23] X. Li, Q. Yang, Y. Zhao, S. Long, J. Zheng, *Soft matter* **2017**, 13, 911.

[24] H. Liu, X. Wang, Y. Cao, Y. Yang, Y. Yang, Y. Gao, Z. Ma, J. Wang, W. Wang, D. Wu, *ACS Appl Mater Interfaces* **2020**, 12, 25334.

[25] Y. Ding, J. Zhang, L. Chang, X. Zhang, H. Liu, L. Jiang, *Advanced materials* **2017**, 29.

[26] J. Xu, R. Jin, L. Duan, X. Ren, G. Gao, *Carbohydr Polym* **2019**, 211, 1.

[27] X. Zhang, N. Sheng, L. Wang, Y. Tan, C. Liu, Y. Xia, Z. Nie, K. Sui, *Materials Horizons* **2019**, 6, 326.

[28] X. Lu, Y. Si, S. Zhang, J. Yu, B. Ding, *Advanced Functional Materials* **2021**, 2103117.

[29] C. Lu, X. Chen, *Nano letters* **2020**, 20, 1907.

[30] X. Jing, H.-Y. Mi, X.-F. Peng, L.-S. Turng, *Carbon* **2018**, 136, 63.

[31] J. Han, H. Wang, Y. Yue, C. Mei, J. Chen, C. Huang, Q. Wu, X. Xu, *Carbon* **2019**, 149, 1.
[32] D. Gan, W. Xing, L. Jiang, J. Fang, C. Zhao, F. Ren, L. Fang, K. Wang, X. Lu, *Nature communications* **2019**, 10, 1487.
[33] Q. Zhou, J. Lyu, G. Wang, M. Robertson, Z. Qiang, B. Sun, C. Ye, M. Zhu, *Advanced Functional Materials* **2021**, 2104536.
[34] S. Chen, L. Sun, X. Zhou, Y. Guo, J. Song, S. Qian, Z. Liu, Q. Guan, E. Meade Jeffries, W. Liu, Y. Wang, C. He, Z. You, *Nature communications* **2020**, 11, 1107.
[35] Q. Zhang, X. Liu, L. Duan, G. Gao, *Chemical Engineering Journal* **2019**, 365, 10.
[36] X. Qu, S. Wang, Y. Zhao, H. Huang, Q. Wang, J. Shao, W. Wang, X. Dong, *Chemical Engineering Journal* **2021**, 425, 131523.
[37] S. Xia, Q. Zhang, S. Song, L. Duan, G. Gao, *Chemistry of Materials* **2019**, 31, 9522.
[38] Q. Zhang, X. Liu, L. Duan, G. Gao, *Journal of Materials Chemistry A* **2021**, 9, 1835.
[39] R. Fu, L. Tu, Y. Zhou, L. Fan, F. Zhang, Z. Wang, J. Xing, D. Chen, C. Deng, G. Tan, P. Yu, L. Zhou, C. Ning, *Chemistry of Materials* **2019**, 31, 9850.
[40] Y. Liu, W. Wang, K. Gu, J. Yao, Z. Shao, X. Chen, *ACS Appl Mater Interfaces* **2021**, 13, 29008.
[41] X. Lei, D. Ye, J. Chen, S. Tang, P. Sun, L. Chen, A. Lu, Y. Du, L. Zhang, *Chemistry of Materials* **2019**, 31, 10032.
[42] J. Y. Sun, X. Zhao, W. R. Illeperuma, O. Chaudhuri, K. H. Oh, D. J. Mooney, J. J. Vlassak, Z. Suo, *Nature* **2012**, 489, 133.
[43] Y. Zhao, B. Zhang, B. Yao, Y. Qiu, Z. Peng, Y. Zhang, Y. Alsaid, I. Frenkel, K. Youssef, Q. Pei, X. He, *Matter* **2020**, 3, 1196.
[44] Z. Wang, J. Chen, L. Wang, G. Gao, Y. Zhou, R. Wang, T. Xu, J. Yin, J. Fu, *Journal of materials chemistry. B* **2019**, 7, 24.
[45] J. Liang, G. Shan, P. Pan, *Soft matter* **2017**, 13, 4148.
[46] W. Ge, S. Cao, Y. Yang, O. J. Rojas, X. Wang, *Chemical Engineering Journal* **2021**, 408, 127306.
[47] Y. Yang, X. Wang, F. Yang, H. Shen, D. Wu, *Advanced materials* **2016**, 28, 7178.
[48] X. Jing, P. Feng, Z. Chen, Z. Xie, H. Li, X.-F. Peng, H.-Y. Mi, Y. Liu, *ACS Sustainable Chemistry & Engineering* **2021**, 9, 9209.
[49] Q. Chen, L. Zhu, C. Zhao, Q. Wang, J. Zheng, *Advanced materials* **2013**, 25, 4171.
[50] Q. Chen, L. Zhu, H. Chen, H. Yan, L. Huang, J. Yang, J. Zheng, *Advanced Functional Materials* **2015**, 25, 1598.
[51] Q. Chen, X. Yan, L. Zhu, H. Chen, B. Jiang, D. Wei, L. Huang, J. Yang, B. Liu, J. Zheng, *Chemistry of Materials* **2016**, 28, 5710.
[52] X. Li, H. Wang, D. Li, S. Long, G. Zhang, Z. Wu, *ACS Appl Mater Interfaces* **2018**, 10, 31198.
[53] M. K. Shin, G. M. Spinks, S. R. Shin, S. I. Kim, S. J. Kim, *Advanced materials* **2009**, 21, 1712.